Hard-x-ray microscopy with Fresnel zone plates reaches 40 nm Rayleigh resolution

Article *in* Applied Physics Letters · March 2008

DOI: 10.1063/1.2857476 · Source: OAI

20 authors, including:

Yong S Chu
Brookhaven National Laboratory
268 PUBLICATIONS **4,177** CITATIONS
SEE PROFILE

Jaemock Yi
Samsung Advanced Institute of Technology
32 PUBLICATIONS **725** CITATIONS
SEE PROFILE

Wah-Keat Lee
Brookhaven National Laboratory
252 PUBLICATIONS **3,083** CITATIONS
SEE PROFILE

Hsuehju Wu
National Taiwan University
2 PUBLICATIONS **167** CITATIONS
SEE PROFILE

Hard-x-ray microscopy with Fresnel zone plates reaches 40 nm Rayleigh resolution

Y. S. Chu,[1] J. M. Yi,[1] F. De Carlo,[1] Q. Shen,[1] Wah-Keat Lee,[1] H. J. Wu,[2] C. L. Wang,[2] J. Y. Wang,[2] C. J. Liu,[2] C. H. Wang,[2] S. R. Wu,[2,3] C. C. Chien,[2,3] Y. Hwu,[2,3,4,5,a)] A. Tkachuk,[6] W. Yun,[6] M. Feser,[6] K. S. Liang,[5] C. S. Yang,[7] J. H. Je,[8] and G. Margaritondo[9]

[1]*Advanced Photon Source, Argonne National Laboratory, Argonne, Illinois 60439, USA*
[2]*Institute of Physics, Academia Sinica, Taipei 115, Taiwan*
[3]*Department of Engineering Science and System, National Tsing Hua University, Hsinchu 300, Taiwan*
[4]*Institute of Optoelectronic Sciences, National Taiwan Ocean University, Keelung 202, Taiwan*
[5]*National Synchrotron Radiation Research Center, Hsinchu 300, Taiwan*
[6]*Xradia Inc., 5052 Commercial Circle, Concord, California 94520, USA*
[7]*Center for Nanomedicine, National Health Research Institutes, Miaoli 350, Taiwan*
[8]*X-ray Imaging Center, Pohang University of Science and Technology, Pohang 790-784, Korea*
[9]*Ecole Polytechnique Fédérale de Lausanne (EPFL), CH-1015 Lausanne, Switzerland*

(Received 28 October 2007; accepted 25 January 2008; published online 12 March 2008)

Substantial improvements in the nanofabrication and characteristics of gold Fresnel zone plates yielded unprecedented resolution levels in hard-x-ray microscopy. Tests performed on a variety of specimens with 8–10 keV photons demonstrated a first-order lateral resolution below 40 nm based on the Rayleigh criterion. Combined with the use of a phase contrast technique, this makes it possible to view features in the 30 nm range; good-quality images can be obtained at video rate, down to 50 ms/frame. The important repercussions on materials science, nanotechnology, and the life sciences are discussed. © *2008 American Institute of Physics*. [DOI: 10.1063/1.2857476]

The advent of high-performance x-ray sources potentially opens the door to x-ray microscopy with excellent spatial resolution.[1–4] However, practically achieving nanometer-scale resolution poses formidable technology challenges in producing the required x-ray lens objectives. Fresnel zone plates (FZPs) are widely used as focusing and magnifying optics devices[5,6] and offer the highest imaging resolution in the entire electromagnetic spectrum.[7] A FZP consists of concentric rings with decreasing width and increasing radius—and the outermost zone width approximately sets the resolution. To achieve sufficient focusing (diffraction) efficiency, the zones must have sufficient thickness, e.g., 1.6 μm for a Au zone plate operating at 8 keV photon energy. The combination of a small zone width and a large thickness constitutes a major fabrication challenge, especially for hard-x-ray FZPs.[8]

In 2006, the Xradia company and the Taiwan National Synchrotron Radiation Research Center in Hsinchu announced a full field FZP lateral resolution below the 100 nm mark.[9,10] Their images demonstrated indeed a Gaussian width resolution near 60 nm in the first order (and later 30 nm in the third order) with 8 kV photons. Our present results establish a FZP resolution level reaching a first order resolution below 40 nm with 8 keV photons and similar resolution levels in the photon energy range of 7–18 keV. We obtained these results using a FZP structure with outmost zone width of 45 nm, a diameter of 80 μm, and an aspect ratio of ~20 (thickness of 900 nm), made out of gold on a silicon nitride membrane.

The x-ray tests were performed on the 32-ID microscopy beamline of the Advanced Photon Source (APS) at the Argonne National Laboratory.[11] Our full-field x-ray transmission microscope (TXM) uses a set of capillary condensers that provide fitting illumination of the object having a numerical aperture matched to a set of zone plate lens objectives. The condensers are elliptically shaped glass capillaries. The inner diameter of 0.9 mm was chosen to maximize the vertical acceptance of the APS undulator beam at 65 m from the source. The estimated monochromatic x-ray flux [through a Si(111) double crystal monochromator] focused by the condenser was 2×10^{11}/s at 8 keV. The high brightness of the APS and the optimized condensers design yielded an excellent imaging throughput of 50 ms/frame with $\sim1\times10^{4}$ charge coupled device counts per pixel.

The microscope system can also operate in a Zernike phase contrast imaging mode with a Au Zernike phase ring placed at the back focal plane of the FZP objective.[12] This phase imaging mode increases the contrast for fine features of most materials in the hard x-ray spectral region—especially materials consisting of low atomic number elements, for which the contrast can increase by two orders of magnitude. This is particularly important for organic and biological specimens. The contrast enhancement is already quite evident when comparing [Figs. 1(a) and 1(b)] an absorption contrast image and a Zernike phase contrast image of the same test pattern taken with 8 keV photons without the standard flat field correction image processing.

Figure 1(c) shows a Zernike contrast image of a 180 nm thick Siemens star test pattern with 30 nm minimum separation at the center. The spatial resolution of the microscope is sufficiently high to visually distinguish the 30 nm feature at the tip of the radial spokes. In order to quantify the resolution level, we fitted intensity line profiles across sharp features in the test pattern using an error function lineshape. An example of such knife-edge intensity profile is shown in Fig. 1(d). A detailed analysis of several test images revealed that

a)Electronic mail: phhwu@sinica.edu.tw

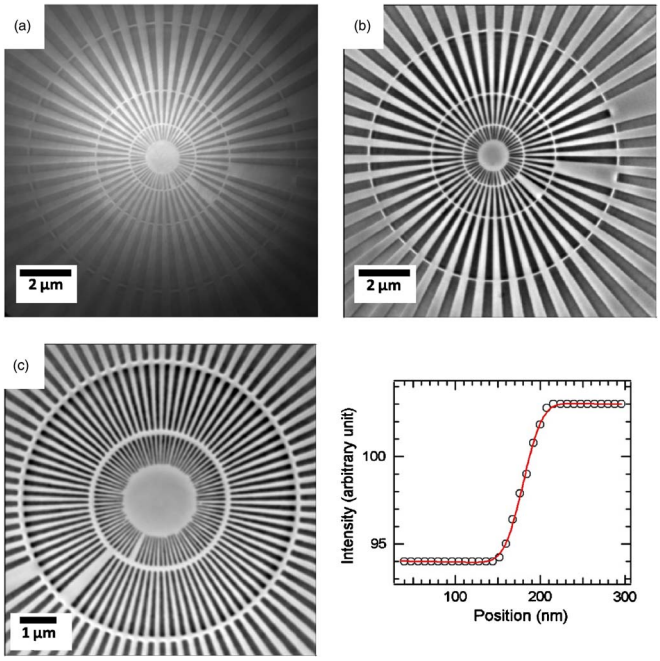

FIG. 1. (Color online) Images (a) and (b) are x-ray micrographs of a 650 nm thick Au Siemens star test pattern with an innermost feature width of 50 nm; (a) is an absorption image and (b) a Zernike phase contrast image. (c) Zernike phase contrast image of a 180 nm thick Au Siemens star test pattern with an innermost feature width of 30 nm. (d) An example of knife-edge intensity profile taken across a sharp feature of the test pattern. The Rayleigh resolution determined from the line profile is 38.5 ± 1.2 nm.

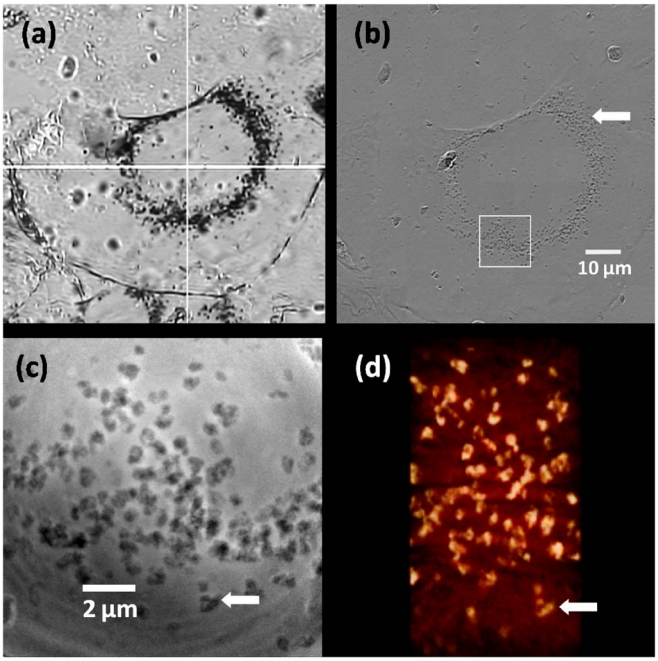

FIG. 2. (Color online) (a) Optical image of an EMT cancer cell cocultured with nanoparticles of gold on a Kapton film. The cross hairs are used for alignment. (b) A 9×9 patchwork of 13×13 μm^2 x-ray micrographs showing the cell shown in (a). (c) An individual micrograph of 13×13 μm^2 field of view indicated by a box in (b). (d) A tomographically reconstructed image of the region shown in (c). The arrow in (c) and (d) points the same agglomerated Au particles.

the knife-edge intensity profile changes from 25% to 75% over a distance of 22.7 ± 0.7 nm. This "25%–75%" linewidth value is related to more frequently used Rayleigh resolution by a factor of 1.7.[13] Thus, our knife-edge line profile result is equivalent to a Rayleigh resolution of 38.5 ± 1.2 nm.

This conclusion is consistent with the results of a modulus transfer function analysis on the same test pattern that yielded a half-period of 38 nm at 26.5% contrast level. The resolution levels so demonstrated are substantially better than previous reports[14,15] and constitute the best current lateral resolution for zone plate hard-x-ray microscopy. The spatial resolution of TXM with an objective zone plate with the minimum zone width Δr is equal to $2k_1\ \Delta r$, where the numerical value of k_1 ranges from 0.3 to 0.61, depending on the illumination condition.[7] Our experimental result corresponds to $k_1 = 0.43$, which is comparable to the previously reported values of 0.4 (Ref. 7) and 0.45.[14]

The conclusions about the resolution and the excellent overall performances were confirmed by a series of other tests on different types of specimens. Figures 2 and 3 show a subset of the results. In Fig. 2, we see images for an EMT6 mouse mammary carcinoma cell cocultured with nanoparticles of gold[16,17] and fixed with glutaraldehyde before dispensed and dried on a Kapton film. Specific images in Fig. 2 are (a) an optical image of the cell, (b) a 9×9 patchwork of 13×13 μm^2 x-ray micrographs, (c) an individual micrograph, and (d) a tomographically reconstructed image of the same region. The tomographic reconstruction was performed with raw projection images taken in an angle range from $-75°$ to $75°$ with $1°$ steps. The reconstruction was performed by a standard filtered-back-projection method.[18]

Overall, the x-ray micrographs of Fig. 2 show not only good spatial resolution but also excellent contrast and a

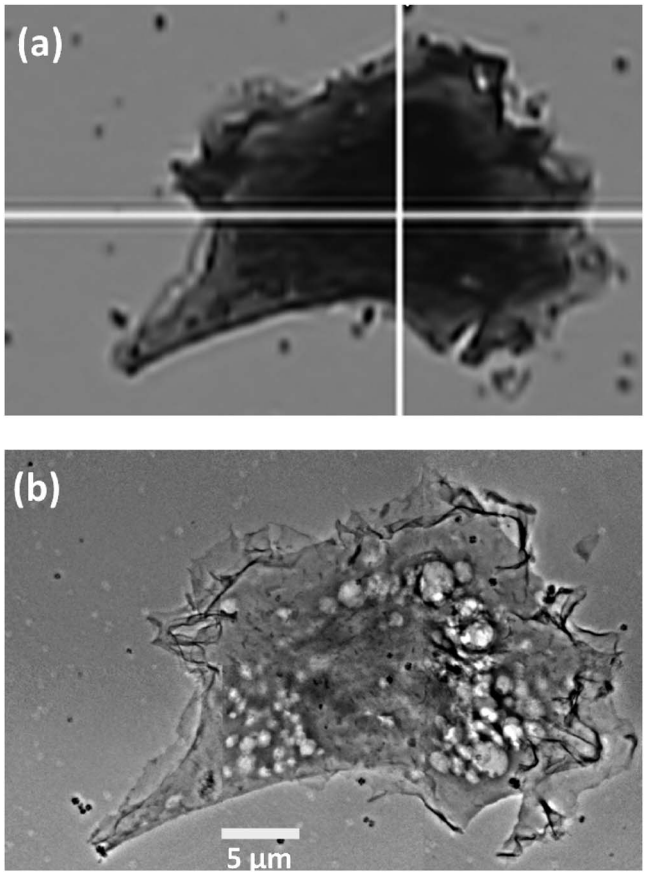

FIG. 3. (a) Optical image and (b) x-ray micrograph of the EMT cell, stained by B521-nickel, allowing the detection of subcellular structures.

wealth of details. Results of this kind are being used to investigate an interesting phenomenon of internalization of gold nanoparticles by cancer cells. Note that cell details like the membrane can be seen. The gold nanoparticles were found to be localized near the nucleus and their size was substantially larger than the original gold particle (~20 nm) indicating that they agglomerated during the internalization process. The agglomeration is also clearly identified in the tomographically reconstructed image of Fig. 2(d).

Figure 3 shows micrographs taken on EMT cells immunostained by B521-nickel and later dehydrated in a graded ethanol series on silicon nitride membrane. The specimen was additionally fixed with osmium tetroxide. The lighter irregular buds known as blebs around nucleus are the lysosomes formed in acidity conditions and during the apoptosis.[19] We see that the staining procedure and the x-ray microscopy resolution make it possible to detect the organelles in the internal cell structure.

These results illustrate a few of the many opportunities opened up by the new resolution levels in x-ray microscopy. Besides subcellular imaging studies in the life sciences, these performances can be used, for example, to images nanostructures of interest in nanoscience and nanotechnology. Preliminary tests were also performed on individual aerosol particles from contaminated urban atmosphere.

As far as future improvements are concerned, we estimate that outermost FZP zone width of 30 nm (Ref. 20) will be feasible in the near future with a possible additional improvement in resolution. Furthermore, the very high flux achieved with our setup makes the practical use of FZPs in the third (or higher) order feasible, with a better resolution even with the present devices. Resolution levels approaching 10 nm can be foreseen: combined with the high penetration of hard x rays, they can open up amazing new opportunities for nondestructive three-dimensional imaging of objects on the nanometer scale.

We acknowledge C. F. Lee for the specimen preparation. This work was supported by National Science and Technology Program for Nanoscience and Nanotechnology, the Thematic Research Project of Academia Sinica, the National Synchrotron Radiation Research Center (Taiwan), the Creative Research Initiatives (Functional X-ray Imaging) of MOST/KOSEF, the Korea Research Foundation Grant (KRF-2007-357-D00140) of MOEHRD (Korea), the Center for Biomedical Imaging (CIBM) in Lausanne, partially funded by the Leenaards and Jeantet foundations and by the Swiss Fonds National de la Recherche Scientifique, and by the EPFL. Use of the Advanced Photon Source is supported by the U.S. Department of Energy, Office of Sciences, Office of Basic Energy Sciences, under Contract No. DE-AC02-06CH11357.

[1] C. K. Gary, H. Park, L. W. Lombardo, M. A. Piestrup, J. T. Cremer, R. H. Pantell, and Y. I. Dudchik, Appl. Phys. Lett. **90**, 181111 (2007).
[2] C. G. Schroer, J. Meyer, M. Kuhlmann, B. Benner, T. F. Günzler, B. Lengeler, C. Rau, T. Weitkamp, A. Snigirev, and I. Snigireva, Appl. Phys. Lett. **81**, 1527 (2002).
[3] T. Wilhein, B. Kaulich, E. Di Fabrizio, F. Romanato, S. Cabrini, and J. Susini, Appl. Phys. Lett. **78**, 2082 (2001).
[4] B. Kaulich, S. Oestreich, M. Salome, R. Barrett, J. Susini, T. Wilhein, E. Di Fabrizio, M. Gentili, and P. Charalambous, Appl. Phys. Lett. **75**, 4061 (1999).
[5] W. Yun, B. Lai, A. Krasnoperova, E. Di Fabrizio, Z. Cai, F. Cerrina, Z. Chen, M. Gentili, and E. Gluskin, Rev. Sci. Instrum. **70**, 3537 (1999).
[6] D. Attwood, *Soft X-Rays and Extreme Ultraviolet Radiation: Principles and Applications* (Cambridge University Press, Cambridge, 1999), pp. 337–394.
[7] W. Chao, B. D. Harteneck, J. A. Liddle, E. H. Anderson, and D. T. Attwood, Nature (London) **435**, 1210 (2005).
[8] T. N. Lo, Y. T. Chen, C. W. Chiu, C. J. Liu, S. R. Wu, I. K. Lin, C. I. Su, W. D. Chang, Y. Hwu, B. Y. Shew, C. C. Chiang, J. H. Je, and G. Margaritondo, J. Phys. D **40**, 3172 (2007).
[9] G. C. Yin, Y. F. Song, M. T. Tang, F. R. Chen, K. S. Liang, F. W. Duewer, M. Feser, W. B. Yun, and H. P. D. Shieh, Appl. Phys. Lett. **89**, 221122 (2006).
[10] P. Y. Tseng, Y. T. Shih, C. J. Liu, T. Hsu, C. C. Chien, W. H. Leng, K. S. Liang, G. C. Yin, F. R. Chen, J. H. Je, G. Margaritondo, and Y. Hwu, AIP Conf. Proc. **879**, 1964 (2007).
[11] Q. Shen, W.-K. Lee, K. Fezzaa, Y. S. Chu, F. De Carlo, P. Jemian, J. Ilavsky, M. Erdmann, and G. G. Long, Nucl. Instrum. Methods Phys. Res. A **582**, 77 (2007).
[12] H. Yokosuka, N. Watanabe, T. Ohigashi, Y. Yoshida, S. Maeda, S. Aoki, Y. Suzuki, A. Takeuchi, and H. Takano, J. Synchrotron Radiat. **9**, 179 (2002).
[13] Y. Horikawa, J. Opt. Soc. Am. A **11**, 1985 (1994).
[14] G. C. Yin, M. T. Tang, Y. F. Song, F. R. Chen, K. S. Liang, F. W. Duewer, W. B. Yun, C. H. Ko, and H. P. D. Shieh, Appl. Phys. Lett. **88**, 241115 (2006).
[15] G. C. Yin, F. Duewer, Y.-F. Song, M.-T. Tang, W. Yun, and K. S. Liang, IPAP Conf. Ser. **7**, 258 (2005).
[16] C. H. Wang, C. C. Chien, Y. L. Yu, C. J. Liu, C. F. Lee, C. H. Chen, Y. Hwu, C. S. Yang, J. H. Je, and G. Margaritondo, J. Synchrotron Radiat. **14**, 477 (2007).
[17] Y. C. Yang, C. H. Wang, Y. K. Hwu, and J. H. Je, Mater. Chem. Phys. **100**, 72 (2006).
[18] A. C. Kak and M. Slaney, *Principles of Computerized Tomographic Imaging* (IEEE, New York, 1988).
[19] K. Glunde, S. E. Guggino, M. Solaiyappan, A. P. Pathak, Y. Ichikawa, and Z. M. Bhujwalla, Neoplasia **5**, 533 (2003).
[20] Y. T. Chen, T. N. Lo, C. W. Chiu, C. J. Liu, S. R. Wu, S. T. Jeng, C. C. Yang, J. Shiue, C. H. Chen, Y. Hwu, G. C. Yin, H. M. Lin, J. H. Je, and G. Margaritondo, J. Synchrotron Radiat. **15**, 170 (2008).